SB^{3}C2017
Summer Biomechanics, Bioengineering and Biotransport Conference
June 21 – 24, Tucson, AZ, USA

HEMODYNAMIC RISK IN CORONARY BIFURCATIONS: A COMPUTATIONAL EXPLORATION

D. Gallo (1), C. Chiastra (2,3), P. Tasso (1), F. Iannaccone (4), F. Migliavacca (2), J.J. Wentzel (3), U. Morbiducci (1)

(1) Department of Mechanical and Aerospace Engineering
Politecnico di Torino
Turin, Italy

(2) Department of Cardiology, Biomedical Engineering
Erasmus MC
Rotterdam, The Netherlands

(3) Laboratory of Biological Structure Mechanics, Department of Chemistry, Materials and Chemical Engineering "Giulio Natta", Politecnico di Milano, Milan, Italy

(4) FEops NV
Ghent, Belgium

INTRODUCTION

The so-called "hemodynamic hypothesis" suggests that local hemodynamics is a main factor of the onset and progression of lesions at arterial bifurcations [1]. Local hemodynamics is mainly determined by the underlying anatomical features of an arterial bifurcation. For example in carotid arteries, computational fluid dynamics (CFD) studies showed a correlation between geometry and disturbed shear [2]. Furthermore, local geometry of carotid bifurcation has been reported to be significantly correlated with peculiar helical flow structures [3], which in turn have been proven to reduce the likelihood of flow disturbances at the bifurcation [4]. While the interplay between geometry, near-wall and intravascular flow features has been widely studied in carotid bifurcations, less is known about diseased coronary bifurcations. Indeed, several studies focused on the influence on near-wall descriptors attributable to anatomical features, such as the presence of stenosis at varying locations and with different severity/extension, bifurcation angle, curvature [5], and tortuosity [6]. The aim of the present study is to extend the investigation of the influence of peculiar coronary bifurcation anatomical features on both near-wall and intravascular flow features. In particular, the impact of stenosis, bifurcation angle, and curvature on local hemodynamics is analyzed by performing CFD simulations on a population-based, idealized model of coronary bifurcation. Such an idealized model-based approach will enable, by varying one specific geometrical feature at time while keeping the others constant, to clearly identify whether and to which extent specific anatomic features promote atherosensitive hemodynamic phenotypes.

METHODS

A parametric model of a coronary bifurcation (Fig.1) representing the left anterior descending (LAD) coronary artery with its diagonal branch was created, as detailed elsewhere [7]. Briefly, the diameter of the proximal main branch (P-MB) is 3.30 mm while the diameters of the distal main branch (D-MB) and the side branch (SB) are 2.77 mm and 2.10 mm, respectively [8].
The distal bifurcation angle was varied within the physiological range. The cardiac curvature was taken into account by bending the model on a sphere of radius 'R'. A physiological cardiac curvature radius was considered (R=56.3 mm), as well as two extreme values (R=∞, i.e. absence of curvature, and R=16.5 mm). Stenosed (diseased) and unstenosed (healthy) bifurcation models were analyzed. Stenosed models are characterized by 60% diameter stenosis in each branch (Medina classification 1,1,1). The lesion is 12 mm long and eccentric, with plaque located at the inner arc of the vessel (Fig. 1).

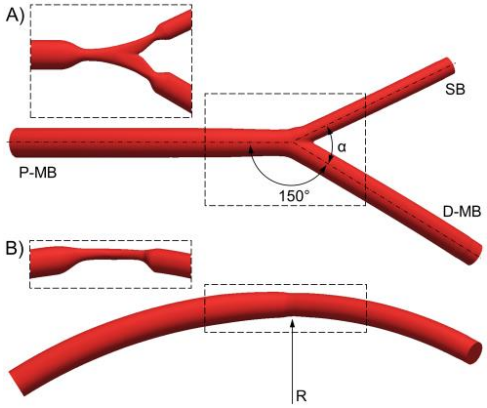

Figure 1 – Parametric model of the healthy left anterior descending / first diagonal coronary bifurcation: (A) top and (B) lateral views. Details of the diseased model are shown in the boxes.

In summary, 10 coronary bifurcation models were investigated by combining 3 distal angles (40°, 55°, and 70°) and 3 curvature radii, both for the healthy and the diseased coronary bifurcation models. The governing equations of unsteady fluid motion were solved by using the finite volume method. A typical human LAD flow waveform was imposed at the inlet as a plug velocity profile. A flow-split of 0.65:0.35 for the D-MB and SB, respectively, was applied at outlets. The flow-split was maintained constant in the diseased models in order to focus the analysis only on the impact that geometrical features have on local hemodynamics. Blood was modeled as a non-Newtonian fluid using the Carreau model. The flow was assumed as laminar (max Reynolds number ~ 330 at the P-MB stenosis of diseased models). Intravascular fluid structures were investigated in terms of helical flow topology and content. Helicity intensity h_2 and helical rotation balance h_4 were calculated, according to [4]:

$$h_2 = \frac{1}{T\,V}\int_T \int_V |\vec{v}\cdot\vec{\omega}|dVdt \quad (1) \qquad h_4 = \frac{\left|\int_T \int_V \vec{v}\cdot\vec{\omega}\, dVdt\right|}{\int_T \int_V |\vec{v}\cdot\vec{\omega}|dVdt} \quad (2)$$

where $\vec{v}$, $\vec{\omega}$ are the velocity and vorticity vectors, respectively, V is the volumetric fluid domain of interest, T is the cardiac cycle. Helicity intensity h_2 is an indicator of the total amount of helical flow, while h_4 measures the strength of relative rotations of helical flow structures. Near-wall hemodynamics was evaluated in terms of time-averaged WSS (TAWSS), oscillatory shear index (OSI), and relative residence time (RRT). In particular, the fraction of the luminal surface area exposed to TAWSS < 0.4 Pa, OSI > 0.2, and RRT > 4.17 Pa^{-1} (in consequence of values set for TAWSS and OSI) was calculated.

RESULTS AND DISCUSSION

The analysis was carried out on the entire bifurcation and single branches. Findings related to the hemodynamic descriptors over the entire bifurcation are summarized in Tables 1 and 2. Generation and transport of helical flow structures is influenced by the curvature radius. Smaller curvature radius is associated with higher helicity intensity in both unstenosed and stenosed cases. In healthy cases, helical flow topology is driven mainly by the curvature of the vessel. In diseased cases, the impact of curvature on helical flow structures piles up with the helicity generated because of the lumen reduction (Fig. 2A). Consequently, helicity intensity h_2 of diseased models is one order of magnitude higher than healthy cases. Globally, helical flow structures are symmetrical, as demonstrated by the nearly 0 values of the helical rotation balance h_4. The surface areas exposed to atherosensitive RRT values can be observed in diseased cases at the distal MB and at the SB, close to the reattachment point of the recirculation regions (Fig. 2B). The curvature radius moderately affects the near-wall hemodynamics of the diseased cases. In particular, smaller curvature radius leads to larger lumen area exposed to low TAWSS and smaller lumen area exposed to high OSI and RRT. The bifurcation angle has a minor effect on the calculated hemodynamic variables. Helicity intensity is not dependent from the bifurcation angle in both healthy and diseased cases. Furthermore, in the healthy cases, the fraction of the lumen surface area exposed to low TAWSS slightly decreases with increasing bifurcation angle, while the exposure to high OSI and RRT is negligible. In the diseased cases, the surface area exposed to low TAWSS increases to ~3.3%. Surface areas exposed to high OSI and RRT show a poor dependence on the bifurcation angle.

In conclusion, the approach proposed in this study provides a controlled benchmark to investigate the effect of various geometrical features on local hemodynamics, highlighting the complex interplay between anatomy and intricate fluid structures in coronary bifurcations.

Table 1 – Near-wall hemodynamic descriptors for cases with different curvature radius 'R'.

Stenosis	R [mm]	Relative surface area [%]			h_2 [m/s^2]	h_4
		TAWSS<0.4Pa	OSI>0.2	RRT>4.17Pa^{-1}		
No	∞	0.00	0.00	0.00	0.20	0.00
	56.3	0.07	0.00	0.00	0.43	0.02
	16.5	0.07	0.00	0.00	1.12	0.00
Yes	∞	2.74	2.08	2.12	4.56	0.01
	56.3	3.21	2.04	2.01	5.13	0.06
	16.5	3.81	1.11	1.56	6.60	0.08

Table 2 – Near-wall hemodynamic descriptors for cases with different bifurcation angles 'α'.

Stenosis	α	Relative surface area [%]			h_2 [m/s^2]	h_4
		TAWSS<0.4Pa	OSI>0.2	RRT>4.17Pa^{-1}		
No	40°	0.42	0.00	0.00	0.43	0.00
	55°	0.07	0.00	0.00	0.43	0.02
	70°	0.00	0.00	0.00	0.44	0.02
Yes	40°	3.35	1.58	2.04	4.58	0.07
	55°	3.31	2.04	2.01	5.13	0.06
	70°	3.24	2.07	2.06	4.85	0.01

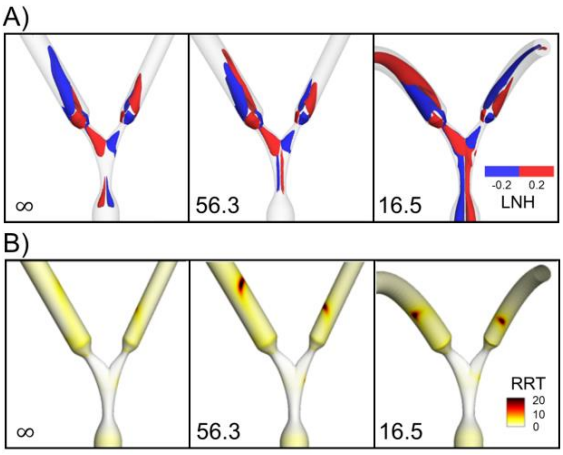

Figure 2 – Hemodynamics results of the diseased cases with different curvature radii: A) Isosurfaces of local normalized helicity (LNH); positive and negative values of LNH indicate counter-rotating flow structures. B) Contour maps of relative residence time (RRT, Pa^{-1}).

ACKNOWLEDGEMENTS

C. Chiastra and J.J. Wentzel are supported by the ERC starting grant (No. 310457, BioCCora).

REFERENCES

[1] Morbiducci, U et al., *Thromb Haemost*, 115(3):484-92, 2016.
[2] Lee, SW et al., *Stroke*, 39:2341–2347, 2008.
[3] Gallo, D et al., *Ann Biomed Eng*, 43:68–81, 2015.
[4] Gallo, D et al., *J Biomech*, 45:2398–2404, 2012.
[5] Peng, C et al., *PLoS One*, 11, e0157490, 2016.
[6] Vorobtsova, N et al., *Ann Biomed Eng*, 44(7):2228-39, 2016.
[7] Chiastra, C et al., *Biomed Eng Online*, 15(1):91, 2016.
[8] Finet, G et al., *EuroIntervention*, 3:490–8, 2008.